Effects of China's Current Air Pollution Prevention and Control Action Plan on Air Pollution Patterns, Health Risks and Mortalities in Beijing 2014-2018

Kamal Jyoti Maji [1, *], Victor OK Li [1, #], Jacqueline CK Lam [1, 2, 3, 4 #]

[1] Department of Electrical and Electronic Engineering, The University of Hong Kong

[2] Energy Policy Research Group, Judge Business School, The University of Cambridge

[3] Department of Computer Science and Technology, The University of Cambridge

[4] CEEPR, MIT Energy Initiative, MIT

[#] Both authors have equal contributions

[*] Corresponding author: Department of Electrical and Electronic Engineering, The University of Hong Kong, Hong Kong, SAR, China

E-mail address: kjmaji@gmail.com (K. J. Maji)

Abstract:

Beijing is one of the most polluted cities in the world. However, the "Air Pollution Prevention and Control Action Plan" (APPCAP), introduced since 2013 in China, has created an unprecedented drop in pollution concentrations for five major pollutants, except O_3, with a significant drop in mortalities across most parts of the city. To assess the effects of APPCAP, air pollution data were collected from 35 sites (divided into four types, namely, urban, suburban, regional background, and traffic) in Beijing, from 2014 to 2018 and analysed. Simultaneously, health-risk based air quality index (HAQI) and district-specific pollution ($PM_{2.5}$ and O_3) attributed mortality were calculated for Beijing. The results show that the annual $PM_{2.5}$ concentration exceeded the Chinese national ambient air quality standard Grade II (35 $\mu g/m^3$) in all sites, ranging from 88.5±77.4 $\mu g/m^3$ for the suburban site to 98.6±89.0 $\mu g/m^3$ for the traffic site in 2014, but was reduced to 50.6±46.6 $\mu g/m^3$ for the suburban site, and 56.1±47.0 $\mu g/m^3$ for the regional background in 2018. O_3 was another most important pollutant that exceeded the

Grade II standard (160 $\mu g/m^3$) for a total of 291 days. It peaked at 311.6 $\mu g/m^3$ in 2014 for the urban site and 290.6 $\mu g/m^3$ in 2018 in the suburban site. APPCAP led to a significant reduction in $PM_{2.5}$, PM_{10}, NO_2, SO_2 and CO concentrations by 7.4, 8.1, 2.4, 1.9 and 80 $\mu g/m^3$/year respectively, though O_3 concentration was increased by 1.3 $\mu g/m^3$/year during the five-years. HAQI results suggest that during the high pollution days, the more vulnerable groups, such as the children, and the elderly, should take additional precautions, beyond the recommendations currently put forward by Beijing Municipal Environmental Monitoring Center (BJMEMC). In 2014, $PM_{2.5}$ and O_3 attributed to 29,270 and 3,030 deaths respectively, though in 2018 their mortalities were reduced by 5.6% and 18.5% respectively. The highest mortality was observed in Haidian and Chaoyang districts, two of the most densely populated areas in Beijing. Beijing's air quality has seen a dramatic improvement over the five-year period, which can be attributable to the implementation of APPCAP and the central government's determination, with significant drops in the mortalities due to $PM_{2.5}$ and O_3 in parallel. To further improve air quality in Beijing, more stringent regulatory measures should be introduced to control volatile organic compounds (VOCs) and reduce O_3 concentrations. Consistent air pollution control interventions will be needed to ensure long-term prosperity and environmental sustainability in Beijing, China's most powerful city. This study provides a robust methodology for analyzing air pollution trends, health risks and mortalities in China. The crucial evidence generated forms the basis for the governments in China to introduce location-specific air pollution policy interventions to further reduce air pollution in Beijing and other parts of China. The methodology presented in this study can form the basis for future fine-grained air pollution and health risk study at the city-district level in China.

Keywords: Beijing; Air Pollution Policy; Sessional-Daily Variation; Trends; Mortality; Vulnerable Group

1. Introduction

Over the past decades, China has experienced rapid industrialization and economic growth and become the world's second-largest economy (WB, 2019). Due to air pollution from industries, urbanization and higher energy consumption, the country has to subsequently take up serious health burden, and associated economic loss (Lelieveld et al., 2015; Zhang et al., 2017; Guan et al., 2019). The Global Burden of Disease (GBD) study estimated that $PM_{2.5}$ exposure led to 852 thousand deaths in China in 2017 (Stanaway et al., 2018) and projected the number of deaths can have reached 2.3 millions by 2030 and 2.7 millions by 2060 (Xie et al., 2019; OECD, 2016). The health burden will significantly impact China's economy, costing about 2% in 2030 and 2.6 % in 2060 of China's GDP (OECD, 2016; Xie et al., 2019). After the 2008 Summer Olympics had been completed in Beijing, air pollution received the highest awareness in China from the public, decision-makers and academic community. Special focus was put on Beijing, the capital of China, which suffered from an extremely high level of $PM_{2.5}$ pollution (Wang et al., 2010; He et al., 2016).

To overcome the air pollution challenge, China's State Council initiated the "Air Pollution Prevention and Control Action Plan" (APPCAP) in 2013 which set the targets to reduce air pollution in most polluted cities across China by 2017 (CSC, 2013). To implement the national APPCAP and further improve air quality, Beijing Municipal Government additionally formulated and released the "Beijing Clean Air Action Plan: 2013-2017", which set a target for the yearly average concentration of $PM_{2.5}$ to fall below the threshold of 60 $\mu g/m^3$ by 2017 (CCICED, 2013). It is of great interest to the government, policymakers and the overall general public to know whether or not Beijing's air quality meets the set targets. However, air quality study in Beijing is complicated by the use of coal for heating and domestic cooking, transport of air pollutants from neighbouring provinces, adverse meteorological conditions during the winter and the high oxidizing power that associates with the complex chemical composition (Li et al., 2017; Lu et al., 2018).

Several studies were conducted to investigate the air pollution in Beijing with limited observational pollutants data, in which the main focus was on the urban site or an entire area with an average of all monitoring stations data (Wang et al., 2018). Zhang et al., (2018) observed the decrease of $PM_{2.5}$ concentration at the urban and the regional background site by 3.40 and 1.16 $\mu g/m^3$/year from 2014 to 2015, based on a single monitoring station in each location. The fine particle explosive growth events, caused by the rapid increase in $PM_{2.5}$ mass concentration over a few hours, steadily decreased from 39 events in 2013 to 19 events in 2017 (Liu et al., 2019), and the number of winter haze days also decreased from 47 days in 2012 to 15 days in

2017 (Dang and Liao, 2019). Based on one urban monitoring data, Cheng et al. (2019) reported that the annual average maximum daily 8-hour average (MDA8-h) O_3 concentration increased from 61.4 $\mu g/m^3$ in 2006 to 96.7 $\mu g/m^3$ in 2017 with an increasing rate of 3.55 $\mu g/m^3$/year. The increasing trend of ozone in Beijing is also reported by Huang et al., (2018). From 2013 to 2015, the 90^{th} percentile of annual average MDA8-h O_3 of Beijing increased from 183.4 to 202.6 $\mu g/m^3$ (BMEPB, 2015). However, during these three years, the annual mean NO_2 concentration decreased from 56 to 50 $\mu g/m^3$ across the urban site (BMEPB, 2015).

The Beijing Municipal Environmental Monitoring Center (BJMEMC) empowered the Chinese citizens by providing the real-time hourly observations data of six air pollutants from 35 monitoring sites to protect their health. Globally, the important indicator to inform the public to take proper outdoor activities is the Air Quality Index (AQI). However, the AQI neglects the synergistic health effects of exposure to multiple air pollutants. Employing the Health-risk based Air Quality Index (HAQI) method associated with exposure to multiple air pollutants and by comparing the AQI and HAQI, Hu et al., (2015) showed that AQI underestimated the health risks associated with exposures to multiple pollutants, especially during the extremely high air pollution days. The air pollution exposure and health impact assessment are state-of-the-art infrastructures to protect citizens from atmospheric pollution and safeguard their health (Shi et al., 2019). However, most of these health risk studies were undertaken at the city-level and underestimated the more fine-grained scale, district-based air pollution control policy development within Beijing itself. The ground-based air quality measurements serve the best data for pollution-attributed district-based mortality estimation (Yin et al., 2017; Maji et al., 2019).

The major objective of this study is to examine the temporal and the spatial variation of six official pollutants based on real-time monitoring data collected at 35 sites across four typical sites in Beijing, for the period of 2014 - 2018. The second objective includes trend analysis, based on the Mann-Kendall test. The health risks associated with six official pollutants are evaluated based on HAQI and the number of district-based pollution-attributed ($PM_{2.5}$ and O_3) premature deaths is also estimated for 16 districts in Beijing. This study provides a robust methodology of analyzing air pollution trends, health risks and mortality in China, the crucial evidence generated forms the basis for policy-makers in China to introduce location-specific air pollution policy interventions to further reduce air pollution in Beijing. The methodology presented in this study can form the basis for future fine-grained air pollution and health risk study at the city-district level in China.

2. Methodology

2.1. Monitoring sites and data sources

Five-year time series (January 2014 to December 2018) of hourly concentrations of $PM_{2.5}$, PM_{10}, O_3, SO_2, NO_2 and CO for Beijing city was downloaded from 35 monitoring stations operated by the BJMEMC (http://beijingair.sinaapp.com/), which had obtained the data from http://pm25.in. Before 2nd April 2014, no data was available for CO, O_3, SO_2 and NO_2. According to the monitoring function, the 35 monitoring stations are divided into 4 categories: the urban environmental monitoring site (12 stations), the suburban environmental monitoring site (11 stations), the regional background transmission site (control site) (7 stations) and the traffic pollution monitoring site (5 stations) (BJMEMC, 2019). Each station contains automated monitoring systems utilized to measure the concentrations of $PM_{2.5}$ and PM_{10} based on the National Environmental Protection Standards (NEPS) HJ 655-2013 (MEP, 2013a), and O_3, SO_2, NO_2 and CO based on the NEPS HJ 193-2013 (MEP, 2013b). All four typical sites are listed in Table S1 and the locations are shown in Fig.1.

The potential quality of all the available data was assessed based on the criteria developed in previous studies (Song et al., 2017; Silver et al., 2018). After screening, if <90% of hourly data was available for the whole time series, it was removed. Based on the above criteria, all the data from the Mentougou suburban site was removed. The hourly data was used to calculate daily, seasonal and yearly averages for the four-type of sites in Beijing. To analyze the five-year time series for monotonic, linear trends, the Mann-Kendall (M-K) test was used to assess the significance of trends, and the Theil-Sen estimator was used to calculate the magnitude of the trend. The R package 'openair' was used to perform for air quality data analysis (R Core Team, 2019; Carslaw and Ropkind, 2012). The M-K nonparametric test is utilized to test for a significant trend. Advantages of the M-K test are: (1) no distributional assumption is made; (2) no assumption of any specific functional form for the behaviour of the data through time is made; and (3) the M-K test is resistant to the effects of outlying observations. The results are not unduly affected by particularly high or low values that occur during the time series.

Fig. 1. Location of the 35 air quality monitoring sites in Beijing (Tian et al., 2019)

2.2. Health-risk based Air Quality Index (HAQI)

Health-risk based air quality indices (HAQI) were proposed in a few studies to include exposure-response characteristics (Hu et al., 2015; Shen et al., 2017). To define a HAQI, the total excess risk (ER) of exposure to multiple pollutants based on Cairncross's concept (Cairncross et al., 2007) was used. In a general form, the excess risk (ER_i) for pollutant i was estimated based on the relative risk (RR_i) of the pollutant, using the following expression:

$$ER_i = RR_i - 1$$

(1)

where $RR_i = \exp[\beta_i(Z_i - Z_{i,0})]$, the exposure-response coefficient (β_i) describes the increased risk of a population associated with a certain health response (such as mortality) when exposed to the pollutant i, Z_i is the concentration of the pollutant and $Z_{i,0}$ is the threshold concentration, below which the pollutant demonstrates no adverse health effects.

For this study, RR values were chosen from the Chinese studies on long-term exposure to air pollution and non-accidental daily mortality of all ages. The RR values are 1.06, 1.0111, 1.0169, 1.02 and 1.0255 per 10 μg/m^3 increase in concentrations of $PM_{2.5}$, PM_{10}, SO_2 and NO_2, respectively, the value is 1.02 per 20 μg/m^3 increase in O_3 concentration and 1.0255 per one mg/m^3 increase in CO concentration (Yang et al., 2013; Zhang et al., 2017; Turner et al., 2016; Atkinson et al., 2018; T. Li et al., 2018).

It was assumed that the air pollution concentration below Chinese Ambient Air Quality Standards (CAAQS) Grade II, posed little or no health risk. Therefore, the CAAQS 24-hour Grade II standard for the six pollutants were used as $Z_{i,0}$ (https://cleanairasia.org/node8163/). However, some studies indicated these values could be regarded as the threshold values, as below which a zero adverse response would be expected (WHO, 2005).

Total ER of all pollutants ER_{total} is the sum of ER_i for the individual pollutants as shown in Eq. (2):

$$ER_{total} = \sum_{i=1}^{n} ER_i = \sum_{i=1}^{n} (RR_i - 1) \tag{2}$$

The equivalent relative risk (RR_i^*) and equivalent concentration (Z_i^*) is defined as Eq. (3) based on the assumption that the ER of a pollutant i is equal to ER_{total} (Hu et al., 2015):

$$ER_{total} = RR_i^* - 1 = \exp[\beta_i (Z_i^* - Z_{i,0})] - 1 \tag{3}$$

The equivalent concentration of i (Z_i^*), incorporating the health effects from all pollutants was used to calculate HAQI based on Eq. (4) and (5):

$$HAQI_i = \frac{(AQI_{high} - AQI_{low})}{(C_{high} - C_{low})} \times (Z_i^* - Z_{i,0}) + AQI_{low} \tag{4}$$

$$HAQI = \max(HAQI_i) \quad i = 1 \; to \; 6 \tag{5}$$

where AQI_{high} is the index breakpoint corresponding to Z_{high}. AQI_{low} is the index breakpoint corresponding to Z_{low}. Z_{high} is the concentration breakpoint that is larger than Z_i^*. Z_{low} is the concentration breakpoint that is smaller than Z_i^*. The reference concentrations for the pollutants in different health categories were provided by the Ministry of Ecology and Environment in China (Hu et al., 2015, see Table S2 in Supplementary Material).

2.3. Health impact assessment

To avoid overestimation of mortality attributed to ambient air pollution, two independent pollutants $PM_{2.5}$ and O_3 were used in the present study. In the first stage, the long-term mortality attributable to pollutant i exposure was calculated based on the epidemiological hazard ratio or relative risk RR_i, which could link the pollutant concentration to negative health effects. Then pollutant-attributed premature deaths were estimated using the equation (Zheng et al., 2017):

$$\Delta Mort_i = [1 - 1/RR_i] \times B_0 \times E_{pop}$$

(6)

where $\Delta Mort_i$ is the excess premature death due to pollutant i exposure for a specific age group; B_0 is the baseline death rate of a specific health outcome at a specific age and E_{pop} is the exposed population number.

The Log-Linear model, a commonly used method to estimate the relative risk RR_i for O_3, were drawn from the past (Pascal et al., 2013; Lin et al., 2017). The model is expressed as:

$$RR_i(Z) = \exp(\beta_i Z), \qquad where\ Z = \max(0, Z_i - Z_{i,0})$$

(7)

where Z_i represents the ambient concentration of pollutant i and with $Z_{i,0}$ represents the threshold concentration of the pollutant, assuming no health risk association below $Z_{i,0}$. β_i is the exposure-response coefficient for pollutant i, can be derived from an epidemiological study. To estimate non-accidental O_3-attributed mortality, RR_i value from cohort study by Turner et al., (2016) was used. District-specific age-specific population and the baseline mortality rate were extracted from Beijing Statistical Yearbook (BMBS, 2018). The present study used 75.2 μg/m^3 as a threshold concentration for O_3, also recommended by Lelieveld et al., (2015).

As $PM_{2.5}$ did not follow the LL exposure-response model, the integrated exposure-response (IER) model was developed by Burnett et al. (2014) for relative risk estimation. The cause-specific *RR* was calculated through Eq. (8);

$$RR_{IER}(Z_a) = \begin{Bmatrix} 1 + \alpha(1 - \exp^{-\gamma(Z_a - Z_0)^{\delta}}), & if\ Z_a > Z_0 \\ 1, & else \end{Bmatrix} \tag{8}$$

where Z_a is the annual average ambient $PM_{2.5}$ concentration; Z_0 is the threshold concentration below which no additional health impacts are calculated; and α, γ and δ are the parameters used to describe the different shapes of the relative risk curve among various diseases (Burnett et al., 2014). The theoretical minimum risk exposure level of 2.4 μg/m^3 is used for the health risk assessment. The age and cause-specific baseline death rates for 2014 to 2017 were downloaded from the GBD study (GBD, 2019). Following the GBD approach, premature deaths due to five causes (IHD, Stroke, COPD, Lung Cancer and ALRI) attributed to $PM_{2.5}$ exposure were calculated for the age group ≥ 25 years and <5 years and for O_3-related non-accidental mortality, the age group ≥25 years were selected.

3. Results and discussion

3.1. Annual and seasonal variation of air pollutants

Table 1 summarizes the annual average concentration of $PM_{2.5}$, O_3, NO_2 and SO_2 in four typical sites in Beijing. The annual $PM_{2.5}$ concentrations exceeded the Chinese national ambient air quality standards (CNAAQS) Grade II (35 $\mu g/m^3$) in all sites in 2014 to 2018 and varied from 88.5±77.4 $\mu g/m^3$ (suburban) to 98.6±89.0 $\mu g/m^3$ (traffic) in 2014, although the range decreased to 50.6±46.6 $\mu g/m^3$ (suburban) to 56.1±47.0 $\mu g/m^3$ (regional background) in 2018. The average seasonal $PM_{2.5}$ concentration was in the order of winter> autumn> spring>summer in the year 2014-2017 (Table 1). In the winter on average higher $PM_{2.5}$ was observed in the regional background (104.8 $\mu g/m^3$) and traffic site (105.4 $\mu g/m^3$) and in the summer on average lower $PM_{2.5}$ is observed in the suburban site (54.3 $\mu g/m^3$) and regional background site (54.2 $\mu g/m^3$). In 2018, the average $PM_{2.5}$ concentration in the spring is higher than winter in all sites due to smog events in March 2018 (Mullin, 2018). The average $PM_{2.5}$ concentration in the spring was 69.2-73.5 $\mu g/m^3$ and 73.7-55.7 $\mu g/m^3$ in the winter in 2018. Predominantly, high $PM_{2.5}$ in the winter in Beijing was mainly attributed to the adverse meteorological conditions like low temperature and lower boundary layer height, less precipitation and weaker wind and solid fuel (coal) combustion for indoor heating (Che et al., 2014; Liu et al., 2019).

The annual average of MDA8-h ozone concentrations (AMDA8-h) was 112.8±65.8 $\mu g/m^3$, 115±63.5 $\mu g/m^3$, 117±62.6 $\mu g/m^3$ and 83.6±50.3 $\mu g/m^3$ in the urban, the suburban, the regional background and the traffic sites in 2014. AMDA8-h O_3 was almost stable from 2015 to 2017 in Beijing (ranging from 94.6±60.5 $\mu g/m^3$ in 2015 to 94.8±57.1 $\mu g/m^3$ in 2017) and further increased to 82.8±50.5 $\mu g/m^3$ (traffic) to 105.4±60.9 $\mu g/m^3$ (suburban) in 2018. O_3 concentration was a little higher in suburban area than others and the lowest was observed in the traffic site. In the traffic site, the dilution of O_3 is due to the higher photochemical reactions with NO_2 and CO, exhaust from vehicles. The seasonal O_3 concentration was in the order of summer>spring>autumn>winter in all the years. In 2014, the average daily maximum 8-h (MDA8-h) ozone was 125.9 $\mu g/m^3$ (traffic) to 167.7 $\mu g/m^3$ (suburban) in the summer and 39.9

μg/m^3 (traffic) to 46.8 μg/m^3 (suburban) in the winter. The MDA8-h ozone has a range from 133.1 μg/m^3 (traffic) to 167.2 μg/m^3 (suburban) in the summer and 45.7 μg/m^3 (traffic) to 60.6 μg/m^3 (background site) in the winter in 2018 (Table 1). The 90th percentile of annual MDA8-h ozone concentrations in Beijing was quite high, at 204.5 μg/m^3 in 2014, and 197.1 μg/m^3 in 2018, which exceeds Grade II Standard (160 μg/m^3) by 23.2%. Lu et al., (2019) pointed out that the ozone concentration in the summer could be attributed to high temperature and low-humidity conditions, inducing an increase of biogenic volatile organic compounds emissions and enhanced ozone production rate.

The annual average NO_2 concentration exceeded the CNAAQS Grade II (40 μg/m^3) in all the years in the urban (range: 55.9±30.8 μg/m^3 in 2014 to 43.6±26.2 μg/m^3 in 2018) and the traffic (range: 82.1±32.7 μg/m^3 in 2014 to 64.4±28.7 μg/m^3 in 2018) sites, whilst NO_2 never exceeded the standard in regional background site (range: 37.9±19.8 μg/m^3 in 2014 to 32.5±17.6 μg/m^3 in 2018). In traffic site, relatively high NO_2 was observed due to NO_x exhaust from vehicles. Generally, NO_2 concentration is higher in the winter and lower in the summer season in all site (Table 1). The annual average SO_2 concentration never exceeded even the CNAAQS Grade I (20 μg/m^3) and gradually decreased from 12.3-16.0 μg/m^3 in 2014 to 5.9-7.6 μg/m^3 in the year 2018.

Table 1. Annual average pollution concentrations from 2014 to 2018 in four-type of sites in Beijing (US, SUB, RBS and TS represent the urban site, the suburban site, the regional background site and the traffic site; concentration unit is in μg/m^3)

3.2. Daily variation

The daily average $PM_{2.5}$, MDA8-h O_3, NO_2 and SO_2 concentration (μg/m^3) from 2014 to 2018 across four typical sites is shown in Fig.2a. $PM_{2.5}$ shows a similar trend across all four typical sites and most of the highest peaks were observed from January to February. $PM_{2.5}$ values remained flat from May to August, then they gradually increased from October to December. In 2014, from January-February, the daily $PM_{2.5}$ concentration dropped gently from a maximum of 378.6-419.4 μg/m^3 to a minimum of 12.2-14.6 μg/m^3 in May-August, then it slowly increased to 330.6-393.6 μg/m^3 during October-December. Whereas in 2018 relatively lower $PM_{2.5}$ concentrations were observed during this time, and the maximum $PM_{2.5}$ concentration was 168.7-184.3 μg/m^3 between January-February, the minimum was 10.0-12.4 μg/m^3 in May-

August and it peaked again at 211.6-258.4 $\mu g/m^3$ in October-December. The most extreme events occurred during November 27th to December 1st and December 19-26th, 2015 was related to the Southeast Asian haze, and the highest $PM_{2.5}$ concentration shoots up to 537.0 μg/m^3 on December 25 (Koplitz et al., 2016; Z. Liu et al., 2019; Dang and Liao, 2019). The Taklimakan Desert in Northwest China witnesses frequent dust storm events, which bring about significant impacts on the downstream air quality (Li et al., 2018), and for that reason, the non-seasonal $PM_{2.5}$ concentration peak was observed during March to May in Beijing (BBC, 2017). The traffic site recorded the maximum number of days (190 days) which exceeded Grade II standard of $PM_{2.5}$ concentration (75 μg/m^3) while suburban site recorded the minimum number of days (169 days) in 2014, and the corresponding number of days decreased to 80 and 71, respectively, in 2018. The total number of days exceeding the Grade II standards for daily average $PM_{2.5}$ during the period 2014-2018 was 626, accounting for 34% of the total number of days. It is important to note that urban and suburban sites have a total of 49 days (with 18 days in 2014 and 15 days in 2015) and 41 days (with 16 days in 2014 and 12 days in 2015), in which $PM_{2.5}$ concentrations were higher than 250.0 μg/m^3, the AQI of these days should be considered as highly unhealthy.

Fig.2b shows the MDA8-h O_3 concentrations across four-type of sites during 2014-2018. Generally, the monthly variability of ground-level O_3 concentrations peaked in May to August (summer) and was the lowest in January, February and December (winter). In 2014, The peak and valley values of ground-level MDA8-h O_3 concentrations in the urban site were 311.6 μg/m^3 and 6.0 μg/m^3, which were reached in May and November, respectively. Whereas in 2018, the maximum of 290.6 μg/m^3 was reached in the suburban site in June and the minimum of 7.3 μg/m^3 was reached in the urban site in December. Relatively low MDA8-h O_3 was observed in the traffic site due to high photochemical reaction rates in higher NO_2 concentration. The total number of days exceeding Grade II standards (160 μg/m^3) for O_3 was 291 during 2014-2018 (63 days in 2014 and 62 days in 2018), accounting for 16% of the total number of days.

Typically, NO_2 exhibits U-shape patterns in a year; lower values in May to August and higher values in January, November and December (Fig.2c). The traffic site showed flatter U-shapes due to continuous vehicular emission of NO_x in the site and the concentration was quite a bit higher than the other sites. In December 2014, the maximum NO_2 concentration was 116.5 μg/m^3 (suburban) to 148.3 μg/m^3 (traffic) and decreased to 77.3 μg/m^3 (regional background) to 102.5

μg/m^3 (traffic) in December 2018. The highest peak was observed during 1st to 6th January 2017, NO_2 concentration reached 146.4-178.9 μg/m^3. The number of days exceeding Grade II standards for daily average NO_2 (80 μg/m^3) during the period 2014-2018 was 152, in which the lowest exceeded days (18 days) was observed in 2018.

Substantially, SO_2 exhibited U-shape patterns in all years; lower values in May to August, and higher values in January, November and December (Fig.2d) in all sites, with higher values in traffic sites. A smooth decreasing trends were observed at all sites, from maximum peaks of 74.0-96.2 μg/m^3 in December 2014 to 13.2-18.8 μg/m^3 in December 2018.

Fig. 2. Daily average pollution concentrations (a: $PM_{2.5}$; b: MDA8-h O_3; c: NO_2; d: SO_2) at the four typical sites in Beijing from 2014 to 2018. (units are μg/m^3) ($PM_{2.5}$ extreme events shown in the box and green horizontal line indicating the Grade II standard).

3.3. Diurnal variation

Fig.3a shows the annual diurnal variation of $PM_{2.5}$ concentrations across four different typical sites from 2014 to 2018 in Beijing. The diurnal variation of $PM_{2.5}$ concentrations was by and large characterized by a "W" type double wave. The morning peak occurred around 08:00 to 11:00, and an afternoon valley between 15:00 to 17:00. The peak in the night appeared after 19:00 or midnight and then gradually decreased in the early hours of the morning. In 2014, the minimum and maximum values of hourly $PM_{2.5}$ were 81.9 μg/m^3 and 99.7 μg/m^3 at 16:00 and 23:00 in the urban site, whereas, in the traffic site, the observed values were 87.3 μg/m^3 and 110.2 μg/m^3, observed at 14:00 and 01:00. As the year progressed, overall $PM_{2.5}$ concentration was decreased and more flat diurnal variation was observed. In 2018, the minimum and maximum values were 49.8 μg/m^3 (at 07:00 and 16:00) and 56.8 μg/m^3 (at 23:00) in the urban site, and 50.3 μg/m^3 (at 16:00) and 59.9 μg/m^3 (at 23:00) in the traffic site.

The morning and evening peaks were attributable in part to the enhanced human activities during the rush hours, and the afternoon valley was mainly attributable to a higher atmospheric mixing layer, which enhanced air pollution diffusion (Martini et al., 2015). It can be observed from Fig. 3b that the diurnal variability showed a strong seasonal variability between the summer and winter for the year 2014 and 2018. In the summer, the average concentration of pollutants was higher during the daytime and reduced at night, which contrasted with the situation in the winter.

In the summer, a peak was observed between 08:00 to 12:00, though a deep valley occurred between 07:00 to 15:00 in the winter. This difference was mainly due to the diverse sources of pollution and their distinct formation mechanisms in different seasons. The air quality in the summer was more affected by human activities, and during the night, with the decrease in human activities, the concentration of pollutants dropped to a lower level. The main factors influencing outdoor air quality during the winter were the transport and diffusion effects of external pollution sources and the burning of indoor biomass for heating (Liu et al., 2019; Shi et al., 2019). The impact of human activities was relatively small and superseded by meteorological conditions in the winter. Therefore, during the night time, the lower atmospheric and stagnant wind conditions aggravated the accumulation of pollutants and increased the $PM_{2.5}$ concentrations (Lang et al., 2017; Zhang & Cao, 2015). Similar seasonal diurnal variations of $PM_{2.5}$ was noted for the year 2014 (Martini et al., 2015).

Fig.3c shows the hourly average diurnal variation of O_3 concentrations during 2014-2018, which was opposite that of the other air pollutants. Ozone concentrations reach a minimum value before sunrise. Around 09:00, along with increases in solar radiation and temperature, photochemical reactions become more active. Ozone concentrations begin to increase, and they peak around 18:00–20:00. The highest peak concentration was observed in Summer. In winter, the peak concentration of ozone appeared earlier, at around 17:00. From 06:00 to 09:00, coinciding with the morning peak traffic, the concentration of NO increases rapidly. Solar radiation is still weak during this period; thus, the concentration of ozone decreases due to titration with NO ($O_3 + NO \rightarrow NO_2 + O_2$). Between 21:00 and 23:00, the concentration of ozone decreases rapidly due to the decrease in solar radiation and titration with NO during evening peak traffic. In the urban site in 2018, the minimum and maximum values of hourly average O_3 concentration were 29.4 $\mu g/m^3$ and 95.2 $\mu g/m^3$, observed at 8.00 and 19:00, respectively. In the traffic site in 2018, the minimum and maximum values were 20.9 $\mu g/m^3$ and 75.5 $\mu g/m^3$, observed at 9:00 and 19:00, respectively. The diurnal variations of O_3 in the summer and winter has undergone a huge shape metamorphosis and the hourly concentration on summer days was significantly higher than those in the winter (Fig.3d). In 2018, the minimum and maximum O_3 in the summer in the urban site were 45.0 $\mu g/m^3$ and 153.8 $\mu g/m^3$ and, in the winter, 27.3 $\mu g/m^3$ and 50.9 $\mu g/m^3$, respectively. Overall, the amplitude of the variation in ozone concentration was increased in 5-years.

The diurnal variation in NO_2 concentrations can be represented by two peaks (Fig.3e) except in the regional background sites. The first peak was at 07:00–8:00 and the second one appeared in 20:00–22:00; the second peak was significantly higher than the first one. In the regional background site, there was a sharp decline at 14:00–15:00 and the peak was reached at 21:00–22:00. The peak in the morning could be attributed to the rush hour traffic and a peak at night might be related to NO_2 accumulation caused by relatively unfavourable weather conditions and high NO emissions (Cheng et al., 2018). Heavy diesel vehicles are allowed to enter the city at night, resulting in a large amount of NO emissions at night (Sun et al., 2013). The shapes of the diurnal variations in each site are different and the overall NO_2 concentration decreased across all the sites from 2014 to 2018. The minimum and maximum values were quite different in the urban site (28.7 $\mu g/m^3$ and 53.1 $\mu g/m^3$ in 2018) and traffic site (50.4 $\mu g/m^3$ and 72.7 $\mu g/m^3$ in 2018). The hourly concentrations of NO_2 during the winter days were significantly higher than those in the summer (Fig. 3f). This phenomenon might be attributable to the difference in meteorological conditions. The decrease of NO_2 concentrations in the afternoon was related to the increase of boundary layer height and an increase in wind speed which results in the dilution of pollutants. With the decrease in NO_2 and CO concentrations in the afternoon, O_3 concentrations increased and it was suggested that the maximum O_3 concentration in the afternoon was mainly due to photochemical reaction under intense solar radiation conditions, leading to the consumption of NO_2 and CO emissions (Shi et al., 2019). A unimodal shape is observed for the annual average diurnal variations of SO_2 (Fig.3g). In the urban area, the minimum hourly average values were observed at 10.8 $\mu g/m^3$ and 4.7 $\mu g/m^3$ in 2014 and 2018 at early morning 06:00 and the maximum values where 17.9 $\mu g/m^3$ and 7.2 $\mu g/m^3$ in 2014 and 2018 during 10:00-13:00. The diurnal variation in the winter was much higher than the summer and each is different in shape (Fig.3h).

Fig. 3. Diurnal variations of $PM_{2.5}$ (a and b), O_3 (c and d), NO_2 (e and f) and SO_2 (g and h) at four typical sites in Beijing. (a, c, e and g for yearly average, and b, d, f and h for the seasonal summer and winter variations in 2014 and 2018)

3.4. The trend of pollutants from 2014 to 2018

The Theil-Sen estimator was used to calculate the magnitude of the long-term trend after accounting for seasonal variations in the data. Fig.4 presents yearly average changes of air pollutant concentrations at the urban, the suburban, the regional background and the traffic sites of Beijing from 2014 to 2018. Specifically, average yearly changes were, for $PM_{2.5}$ (-7.7, -7.0, -6.3 and -8.4 $\mu g/m^3$/year for the urban, the suburban, the regional background and the traffic sites, respectively), NO_2 (-2.7, -1.7, - 1.4 and -3.9 $\mu g/m^3$/year), MDA8-h O_3 (1.7, 2.0, -0.9 and 2.5 $\mu g/m^3$/year), SO_2 (-2.1, -1.4, -1.9 and -2.2 $\mu g/m^3$/year), PM_{10} (-9.6, -7.9, -5.1 and -9.7 $\mu g/m^3$/year) and CO (-0.07, -0.08, -0.06 and -0.11 mg/m^3/year). The error on the bar shows the minimum and maximum yearly change with 95% confidence interval (95% CI). Fig.4 shows that the air pollution action plan has significantly ameliorated the air quality of Beijing at all four-type of sites, especially for $PM_{2.5}$ and PM_{10}, whereas, except for the regional background site, MDA8-h O_3 increased significantly in all sites. The Action Plan also led to a decrease in SO_2 and NO_2 but to a lesser extent than that of CO, $PM_{2.5}$ and PM_{10}, indicating that SO_2 and NO_2 were significantly affected by other less well-controlled sources. The urban and the traffic sites showed a bigger decrease in $PM_{2.5}$, PM_{10}, NO_2 and SO_2 concentrations in comparison to the other sites. After accounting for seasonal variations, MDA8-h showed a positive trend, although annual average MDA8-h O_3 concentration decreased during the study period, this was due to the increase of summer MDA8-h value.

Cheng et al., (2016) reported the increase of MDA8-h O_3 in the urban area by 2.2 $\mu g/m^3$/year, and a slight decrease at background station by 0.9 $\mu g/m^3$/year from 2004 to 2015. Vu et al., (2019) estimated the annual average levels of $PM_{2.5}$, PM_{10}, SO_2, NO_2 and CO decreased by 7.4, 7.6, 3.1, 2.5 and 94 $\mu g/m^3$/ year, respectively, whereas the level of O_3 increased by 1.0 $\mu g/m^3$/year during 2013 to 2017. The higher decreasing rate of $PM_{2.5}$ was observed in the urban areas in North China, by 10 $\mu g/m^3$/ year during 2013-2017 (Li et al., 2020). The ozone increases in Beijing were largely due to higher background ozone driven by urban heat island effects and increase in summertime biogenic emissions of VOCs and NOx (Lu et al., 2019; Cheng et al., 2019; Chen et al., 2019). However, Li et al., (2019) argued that the decrease of $PM_{2.5}$ contributes more than the decrease of NO_x or VOCs emissions to ozone increasing trends in China, and this is mainly due to aerosol chemistry rather than photolysis.

Fig. 4. The trend of pollutants from 2014 to 2018 (mean values with error bars represent 95% confidence intervals; unit in μg/m^3/year for $PM_{2.5}$, O_3, NO_2, SO_2 and PM_{10}, and in mg/m^3/year for CO).

The trend of ozone in only positive in Beijing and there are various reasons: (a) The biogenic VOCs emissions alone enhance surface DMA8 ozone by more than 29.4 μg/m^3 over central-eastern China in July-August, mainly driven by high temperatures (X. Lu et al., 2019). (b) The precursor material from long-distance transport has the largest contribution to ambient ozone in some provinces in China. The emission rate of precursors in Beijing has decreased, however, the VOCs from nearby areas still make the surface ozone concentration rise (Gao et al., 2019). (c) Reduced $PM_{2.5}$ levels also plausibly cause an increase in O_3 level due to impacts on ozone photochemistry and heterogeneous chemistry on aerosol surfaces. Primarily $PM_{2.5}$ scavenges the hydroperoxy (HO_2) and NO_x radicals that would otherwise produce O_3 (Wang et al., 2019). (d) Also, meteorological conditions were dominant drivers of the ground ozone concentrations, as the surface temperature. Compared to the previous year's summer of 2017 had hotter and drier weather conditions, which promoted ozone production and led to higher ozone levels in 2017 in North China Plain (Ding et al., 2019a).

3.5. Health-risk-based AQI (HAQI)

The exposure-response coefficient characterizes the relationship of pollutants exposure and corresponding additional mortality health risk due to the six pollutants when their concentrations are higher than CAAQS Grade II. Although some adverse health impacts may still exist below the CAAQS Grade II standard, the impact is much smaller (WHO, 2005). Fig.5a shows the percentage of total average ER values for all pollutants in four regions in Beijing from 2014 to 2018. For the six pollutants, $PM_{2.5}$ and PM_{10} were the two major pollutants that contributed the highest percentage of total ER, $PM_{2.5}$ contributed 71.5% (in the suburban area) to 81.5% (in the traffic area) and PM_{10} contributed 9.9% (background site) to 14.1% (traffic site). The average contributions by O_3, NO_2 and CO were 5.4%, 4.2% and 2.6% of total ER, respectively, although their health effects were also significant. The results reveal that $PM_{2.5}$ is the top threat to public health regarding non-accidental mortality among the pollutants.

Each day (from the year 2014 to 2018) is classified into five risk categories based on AQI. The classification of the category on a certain day could change if based on HAQI (Fig.5b). There is no misclassification when AQI is less than 100 (AQI-based health days), as HAQI is equal to AQI. The number of days having good-to-moderate (AQI: 0-100) and hazardous (AQI: > 300) health risk in regional background site was 974 and 47, and in the traffic site, 894 and 67 days. In this context, the air quality was healthier in the regional background site than in the traffic site. For AQI-based light pollution days (100 < AQI<150), 82, 9.4 and 8.5% of days and 77.5, 13.4 and 9.1% of days would be 'unhealthy for sensitive groups', 'unhealthy' and 'very unhealthy' pollution based on HAQI values in the urban and the traffic site, respectively. In moderate pollution days (AQI: 151-200), 39.3, 25.6 and 35.2% of days and 31.7, 10.8 and 57.5% of days would be 'unhealthy', 'very unhealthy' and 'hazardous' pollution days based on HAQI values in the urban and the traffic sites, respectively. And in serious days (AQI: 201-300), above 88% of the days would be 'hazardous' based on HAQI in all sites. In this perspective, the results detect that the health risks are underestimated based on simple AQI system in many days. The public is exposed to multiple pollutants on most pollution days, while AQI captures only the single pollutant with the 'greatest health risk', neglecting the mortality risk of other pollutants. From 2014 to 2018, the average HAQI value decreased around 6% per year.

Fig. 5. (a) Percentage of the excessive risk of pollutants from 2014 to 2018. (b) Comparison of the HAQI-classified health risk categories with the AQI-classified categories (with the average number of days in different ranges; the sum of all year data was included in the analysis).

3.6. Air pollutants-attributed total premature mortality

The $PM_{2.5}$ and O_3 exposure levels vary significantly throughout the year due to both naturogenic reasons such as meteorology and to anthropogenic emissions like transport. Therefore, based on the daily data the Monte Carlo simulation of $PM_{2.5}$ and O_3 were used to calculate district wise pollution concentration in Beijing. Fig.6 (a and b) represents the district wise 5-year annual average $PM_{2.5}$ and O_3 concentration in Beijing and shows a substantial spatial heterogeneity, where $PM_{2.5}$ pollution was high in the central and southern parts and O_3 pollution was high in the northern parts of Beijing. In 2014, $PM_{2.5}$ and O_3 attributed total deaths were 29.27 (95% CI: 18.79–35.4) thousands and 3.03 (95% CI: 1.54–5.9) thousands (Fig.6 c and e). After five years, the estimated number of deaths by $PM_{2.5}$ and O_3 decreased by 5.6% and 18.5% (Fig.6 d and f). In $PM_{2.5}$-attributed mortality, ischemic heart disease (IHD), cerebrovascular disease (Stroke), chronic obstructive pulmonary disease (COPD), lung cancer (LC) among adults (age$\geq$ 25 years), and acute lower respiratory infection (ALRI) in children (age$\leq$5 years) contributed to 37.4, 49.0, 7.2, 6.3 and 0.2%, respectively. It should be noted in Table 2, that premature death is directly proportional to the population size. In Fig.6 (a) shows that $PM_{2.5}$ pollution was higher in Daxing, Fangshan and Tongzhou districts while the total $PM_{2.5}$-attributed deaths in these districts were smaller than those in Haidian, Fengtai and Chaoyang districts due to differences in population distribution across these districts (Fig.S12 and Table 2). The highest premature deaths (due to $PM_{2.5}$ and O_3) were observed in Haidian (5364 in 2014 and 4653 in 2018) and Chaoyang (5751 and 5049) and the lowest deaths were observed in Yanqing (484 and 462) and Mentougou (477 and 461). More details have been reported in Table S4 and Table S5 (Supplementary Material). Even though the pollutant concentrations were substantially reduced in these five years, the total attributed deaths were not reduced, as the total mortality rate, population and aged population ($\geq$25 years) were increased by 5.28, 0.93 and 5.01%, respectively. The cities of Tianjin and Hebei in the Beijing-Tianjin-Hebei (BTH) region, showed a 2.35% decrease and a 15.7% increase in premature deaths from 2010 to 2015 (Zhu et al., 2019). Zhang et al. (2019) reported a 17.2% decrease in total non-accidental mortality in China during 2013-2017, whereas Ding et al., (2019b) reported 20.7% decrease of cause-specific mortality during the same period, although Wu et al. (2019) observed almost no decrease in the number of $PM_{2.5}$-related premature deaths in the Pearl River Delta region from 2006 to 2015.

Fig. 6. District-specific (a) annual average $PM_{2.5}$ concentration ($\mu g/m^3$), (b) annual average O_3 concentration ($\mu g/m^3$) in Beijing from 2014 to 2018, $PM_{2.5}$-attributed premature mortality for the year (c) 2014 and (d) 2018, and O_3-attributed premature mortality for the year (c) 2014 and (d) 2018.

Note: DAX, MEN, HAI, MIY, YAN, HUA, PIN, SHI, FEN, DON, SHU, FAN, CHA, XIC, CHA and TON refer to the districts of Daxing, Mentougou, Haidian, Miyun, Yanqing, Huairou, Pinggu, Shijingshan, Fengtai, Dongcheng, Shunyi, Fangshan, Chaoyang, Xicheng, Changping and Tongzhou

Table 2. Cause-specific premature deaths attributed to $PM_{2.5}$ and O_3 in 16 districts in Beijing

Very few district-specific health risk assessment works have been done in the past, Yin et al. (2017) estimated the maximum and minimum $PM_{2.5}$-attributed deaths at 1773 in Chaoyang and 113 in Yanqing in 2012. At the city-level, $PM_{2.5}$-related reported deaths were 20.9 thousands (Song et al., 2017) and 25.5 thousands (Li et al., 2018) in 2015, 17.7 thousands (Anenberg et al., 2019) and 18.2 thousands in 2016 (Maji et al., 2018), 25.8 thousands in 2017 (Ding et al., 2019b). Ozone-related total reported deaths were 2.98 thousands in 2015 (Xiang et al., 2019) and 2.1 thousands in 2016 (Maji et al., 2019). This difference in estimated pollution attributed deaths is mainly due to different methodologies for estimating death and ground-level ozone, and exposure-response coefficient. Most of the past studies used the average mortality rate and age group population values for China as a whole, which were very different from the district-based values. For example, in 2017, the average mortality rate in Beijing was 6.2%, while the mortality rates in Miyun and Changping districts were 9.5% and 3.4%.

4. Policy implications

Air quality improvement is important for the future prosperity and sustainability of China's most powerful city, Beijing. This improvement in air quality did not happen by chance. It was the result of an enormous investment of time, resources and political will. In 1998 Beijing declared war on air pollution. The challenge was to find ways to improve air quality in one of the largest and fastest-growing cities in the developing world. Air pollution issue in Beijing is partially due to the energy source, especially the higher use of solid and liquid fuel problems in the current stage in China. On the one hand, actions of energy conservation and low-carbon energy transitions to reduce CO_2 emissions also reduce other co-emitted air pollutants, bringing co-benefits for air quality (Zhang et al., 2016). In this study, we emphasize the effects of past air pollution control and action plan to improve the current environmental situation in Beijing, even though $PM_{2.5}$ concentration did not achieve the national standard and O_3 concentration continued to increase due to growing VOC emissions in Beijing. The Chinese government should strengthen the co-governance policy design in the future to achieve maximal effects with minimal economic loss. In summary, in this study, we provide a comprehensive assessment of the air quality in urban, suburban and traffic areas in Beijing, and districts level health burden, which is valuable for policymakers. Now the Beijing authority should develop new district-based policy, on (1) motor vehicle pollution control by using green transportation, (2) coal-fired pollution control by using green energy, (3) key polluted industries control by strengthening the air quality standard, (4) fugitive dust pollution control by using urban green infrastructure, and (5) new technology application in environmental protection, for near-term air quality targets achievement.

5. Conclusion

In this study, data for six official air pollutants are analyzed in 35 monitoring sites (divided into four types, respectively, the urban, the suburban, the regional background, and the traffic site) in Beijing based on the data from 2014 to 2018. None of the 35 sites has met the Grade II Chinese ambient air quality standards for $PM_{2.5}$. The minimum annual average $PM_{2.5}$ was observed in the Badaling monitoring site (68.8 $\mu g/m^3$) in 2014 and the Miyun Reservoir site (45.1 $\mu g/m^3$) in 2018, and the maximum was observed at 125.3 $\mu g/m^3$ in 2014 and 72.2 $\mu g/m^3$ in 2018 in the Liuli River site. The highest peak was observed in late December 2015 during the Southeast Asian haze. During the 626 days or almost half of the five-year studied period, $PM_{2.5}$ concentration had consistently exceeded the Grade II standard. O_3 also exceeded the Grade II standard for 291 days, which peaks at 311.6 $\mu g/m^3$ (in May) in 2014 and 290.6 $\mu g/m^3$ (in June) in 2018. Very high seasonal variations were observed for all six pollutants. The stagnant meteorological conditions and the use of fossil fuels for indoor heating accounted for the high $PM_{2.5}$ concentration in the winter. The decreasing trends were observed for $PM_{2.5}$, PM_{10}, NO_2, SO_2 and CO, whereas, O_3 increased during this time. Among the six pollutants, $PM_{2.5}$ was the major threat to public health and the health risks were underestimated based on the current simple AQI reporting system. From 2014 to 2018, the change of $PM_{2.5}$ and O_3 attributed mortality is low, mainly due to the increase of total mortality rate, the population as well as the aged population. The diurnal variation can be a good source of information for a person's exposure assessment during an outdoor visit. Future research can focus on the chemical composition and source apportionment of fine particles, urban meteorology during haze and photochemistry for Beijing for a longer time. Furthermore, to improve the quality of life, the authorities in Beijing may want to impose even more stringent and effective pollutant control measures, specifically targeting at the most polluted districts in Beijing, such as Chaoyang and Haidian, with priority given to controlling VOCs and industrial pollution in Beijing and the nearby urban regions.

Acknowledgements

This research is supported in part by the Theme-based Research Scheme of the Research Grants Council of Hong Kong, under Grant No. T41-709/17-N. We would like to acknowledge the Beijing Municipal Environment Monitoring Center and National Meteorological Information Center, China for publicizing air quality and meteorological data of Beijing. We would also like to thank Mr Han Yang, PhD student of Electrical and Electronic Engineering, and HKU-Cambridge Clean Energy and Environment Research Platform (CEERP), and HKU-Cambridge AI to Advance Well-being and Society Research Platform (AI-WiSe), the University of Hong Kong, for providing the valuable air quality dataset.

References

Anenberg, S.C., Achakulwisut, P., Brauer, M., Moran, D., Apte, J.S., Henze, D.K., 2019. Particulate matter-attributable mortality and relationships with carbon dioxide in 250 urban areas worldwide. Scientific Reports 9, 11552. https://doi.org/10.1038/s41598-019-48057-9

Atkinson, R.W., Butland, B.K., Anderson, H.R., Maynard, R.L., 2018. Long-term Concentrations of Nitrogen Dioxide and Mortality. Epidemiology 29, 460–472. https://doi.org/10.1097/EDE.0000000000000847

BBC, 2017. Dust storm chokes Beijing and northern China. (Available at: https://www.bbc.com/news/world-asia-china-39801555).

BJMEMC, 2019. Beijing Municipal Environmental Monitoring Center, Beijing Air Quality Automatic Monitoring System. (Available at: http://www.bjmemc.com.cn/xgzs_getOneInfo.action?infoID=1661)

BMEPB, 2015. Beijing Environmental Statement Beijing Municipal Environmental Protection Bureau (2015) (Available at: http://www.bjepb.gov.cn/2015zt_jsxl/index.html)

BMBS, 2018. Annual Data, Beijing Municipal Bureau of Statistics (Available at: http://tjj.beijing.gov.cn/English/AD/)

Cairncross, E.K., John, J., Zunckel, M., 2007. A novel air pollution index based on the relative risk of daily mortality associated with short-term exposure to common air pollutants. Atmospheric Environment 41, 8442–8454. https://doi.org/10.1016/j.atmosenv.2007.07.003

Carslaw, D.C., Ropkins, K., 2012. openair — An R package for air quality data analysis. Environmental Modelling

& Software 27–28, 52–61. https://doi.org/10.1016/j.envsoft.2011.09.008

CCICED, 2013. China Council for International Corporation on environment and Development, Beijing publishes 2013-2017 Clean Air Action Plan. (Available at: http://www.cciced.net/cciceden/NEWSCENTER/LatestEnvironmentalandDevelopmentNews/201310/t20131022_82587.html)

Chen, Z., Zhuang, Y., Xie, X., Chen, D., Cheng, N., Yang, L., Li, R., 2019. Understanding long-term variations of meteorological influences on ground ozone concentrations in Beijing During 2006–2016. Environmental Pollution 245, 29–37. https://doi.org/10.1016/j.envpol.2018.10.117

Cheng, N., Li, R., Xu, C., Chen, Z., Chen, D., Meng, F., Cheng, B., Ma, Z., Zhuang, Y., He, B., Gao, B., 2019. Ground ozone variations at an urban and a rural station in Beijing from 2006 to 2017: Trend, meteorological influences and formation regimes. Journal of Cleaner Production 235, 11–20. https://doi.org/10.1016/j.jclepro.2019.06.204

Cheng, N., Li, Y., Chen, C., Cheng, B., Sun, F., Wang, B., Li, Q., Wei, P., 2018. Ground-Level NO2 in Urban Beijing: Trends, Distribution, and Effects of Emission Reduction Measures. Aerosol and Air Quality Research 18, 343–356. https://doi.org/10.4209/aaqr.2017.02.0092

Cheng, N., Li, Y., Zhang, D., Chen, T., Sun, F., Chen, C., Meng, F., 2016. Characteristics of Ground Ozone Concentration over Beijing from 2004 to 2015: Trends, Transport, and Effects of Reductions. Atmospheric Chemistry and Physics Discussions 1–21. https://doi.org/10.5194/acp-2016-508

CSC, 2013. China's State Council, Notice of the State Council on Printing and Distributing an Action Plan for the Prevention and Control of Air Pollution. (Available at: http://www.gov.cn/zwgk/2013-09/12/content_2486773.htm).

Dang, R., Liao, H., 2019. Severe winter haze days in the Beijing-Tianjin-Hebei region from 1985–2017 and the roles of anthropogenic emissions and meteorological parameters. Atmospheric Chemistry and Physics Discussions 1–31. https://doi.org/10.5194/acp-2019-306

Ding, D., Xing, J., Wang, S., Chang, X., Hao, J., 2019a. Impacts of emissions and meteorological changes on China's ozone pollution in the warm seasons of 2013 and 2017. Frontiers of Environmental Science & Engineering 13, 76. https://doi.org/10.1007/s11783-019-1160-1

Ding, D., Xing, J., Wang, S., Liu, K., Hao, J., 2019b. Estimated Contributions of Emissions Controls, Meteorological Factors, Population Growth, and Changes in Baseline Mortality to Reductions in Ambient PM2.5 and PM2.5-Related Mortality in China, 2013–2017. Environmental Health Perspectives 127, 067009. https://doi.org/10.1289/EHP4157

Gao, M., Gao, J., Zhu, B., Kumar, R., Lu, X., Song, S., Zhang, Y., Wang, P., Beig, G., Hu, J., Ying, Q., Zhang, H., Sherman, P., McElroy, M., 2019. Ozone Pollution over China and India: Seasonality and Sources. Atmospheric Chemistry and Physics Discussions 2, 1–29. https://doi.org/10.5194/acp-2019-875

Guan, Y., Kang, L., Wang, Y., Zhang, N.-N., Ju, M.-T., 2019. Health loss attributed to PM2.5 pollution in China's cities: Economic impact, annual change and reduction potential. Journal of Cleaner Production 217, 284–294. https://doi.org/10.1016/j.jclepro.2019.01.284

GBD, 2019. Global Burden of Disease, IHME Data, GBD Results Tool (Available at: http://ghdx.healthdata.org/gbd-results-tool)

He, G., Fan, M., Zhou, M., 2016. The effect of air pollution on mortality in China: Evidence from the 2008 Beijing Olympic Games. Journal of Environmental Economics and Management 79, 18–39. https://doi.org/10.1016/j.jeem.2016.04.004

Hu, J., Ying, Q., Wang, Y., Zhang, H., 2015. Characterizing multi-pollutant air pollution in China: Comparison of three air quality indices. Environment International 84, 17–25. https://doi.org/10.1016/j.envint.2015.06.014

Huang, J., Pan, X., Guo, X., Li, G., 2018. Health impact of China's Air Pollution Prevention and Control Action

Plan: an analysis of national air quality monitoring and mortality data. The Lancet Planetary Health 2, e313–e323. https://doi.org/10.1016/S2542-5196(18)30141-4

Lang, J., Zhang, Y., Zhou, Y., Cheng, S., Chen, D., Guo, X., Chen, S., Li, X., Xing, X., Wang, H., 2017. Trends of PM2.5 and Chemical Composition in Beijing, 2000–2015. Aerosol and Air Quality Research 17, 412–425. https://doi.org/10.4209/aaqr.2016.07.0307

Lelieveld, J., Evans, J.S., Fnais, M., Giannadaki, D., Pozzer, A., 2015. The contribution of outdoor air pollution sources to premature mortality on a global scale. Nature 525, 367–371. https://doi.org/10.1038/nature15371

Li, J., Liu, H., Lv, Z., Zhao, R., Deng, F., Wang, C., Qin, A., Yang, X., 2018. Estimation of PM2.5 mortality burden in China with new exposure estimation and local concentration-response function. Environmental Pollution 243, 1710–1718. https://doi.org/10.1016/j.envpol.2018.09.089

Li, K., Jacob, D.J., Liao, H., Shen, L., Zhang, Q., Bates, K.H., 2019. Anthropogenic drivers of 2013–2017 trends in summer surface ozone in China. Proceedings of the National Academy of Sciences 116, 422–427. https://doi.org/10.1073/pnas.1812168116

Li, M., Wang, L., Liu, J., Gao, W., Song, T., Sun, Y., Li, L., Li, X., Wang, Yonghong, Liu, L., Daellenbach, K.R., Paasonen, P.J., Kerminen, V.-M., Kulmala, M., Wang, Yuesi, 2020. Exploring the regional pollution characteristics and meteorological formation mechanism of PM2.5 in North China during 2013–2017. Environment International 134, 105283. https://doi.org/10.1016/j.envint.2019.105283

Li, T., Zhang, Y., Wang, J., Xu, D., Yin, Z., Chen, H., Lv, Y., Luo, J., Zeng, Y., Liu, Y., Kinney, P.L., Shi, X., 2018. All-cause mortality risk associated with long-term exposure to ambient PM2·5 in China: a cohort study. The Lancet Public Health 3, e470–e477. https://doi.org/10.1016/S2468-2667(18)30144-0

Liu, Y., Zheng, M., Yu, M., Cai, X., Du, H., Li, J., Zhou, T., Yan, C., Wang, X., Shi, Z., Harrison, R.M., Zhang, Q., He, K., 2019. High-time-resolution source apportionment of PM2.5; in Beijing with multiple models. Atmospheric Chemistry and Physics 19, 6595–6609. https://doi.org/10.5194/acp-19-6595-2019

Liu, Z., Hu, B., Ji, D., Cheng, M., Gao, W., Shi, S., Xie, Y., Yang, S., Gao, M., Fu, H., Chen, J., Wang, Y., 2019. Characteristics of fine particle explosive growth events in Beijing, China: Seasonal variation, chemical evolution pattern and formation mechanism. Science of The Total Environment 687, 1073–1086. https://doi.org/10.1016/j.scitotenv.2019.06.068

Lu, X., Zhang, L., Chen, Y., Zhou, M., Zheng, B., Li, K., Liu, Y., Lin, J., Fu, T.-M., Zhang, Q., 2019. Exploring 2016–2017 surface ozone pollution over China: source contributions and meteorological influences. Atmospheric Chemistry and Physics 19, 8339–8361. https://doi.org/10.5194/acp-19-8339-2019

Maji, K.J., Arora, M., Dikshit, A.K., 2018. Premature mortality attributable to PM2.5 exposure and future policy roadmap for ‘airpocalypse’ affected Asian megacities. Process Safety and Environmental Protection 118, 371–383. https://doi.org/10.1016/j.psep.2018.07.009

Maji, K.J., Ye, W.-F., Arora, M., Nagendra, S.M.S., 2019. Ozone pollution in Chinese cities: Assessment of seasonal variation, health effects and economic burden. Environmental Pollution 247, 792–801. https://doi.org/10.1016/j.envpol.2019.01.049

MEP, 2013a. MEP Technical Specifications for Installation and Acceptance of Ambient Air Quality Continuous Automated Monitoring System for PM10 and PM2.5. Ministry of Environmental Protection, Beijing, China (2013), p. 25 (available at: http://english.mee.gov.cn/Resources/standards/Air_Environment/).

MEP, 2013b. MEP, Technical Specifications for Installation and Acceptance of Ambient Air Quality Continuous Automated Monitoring System for SO2, NO2, O3 and CO. Ministry of Environmental Protection, Beijing, China (2013), p. 27. (available at: http://english.mee.gov.cn/Resources/standards/Air_Environment/).

Mullian., K., 2018. Beicology: Beijing's Recent Smog Resurgence, Explained. (Available at: https://www.thebeijinger.com/blog/2018/05/05/beicology-beijings-recent-smog-resurgence-explained)

OECD, 2016. The Economic Consequences of Outdoor Air Pollution. OECD.

https://doi.org/10.1787/9789264257474-en

R Core Team, 2019. R: A Language and Environment for Statistical Computing. R Foundation for Statistical Computing, Vienna, Austria.

San Martini, F.M., Hasenkopf, C.A., Roberts, D.C., 2015. Statistical analysis of PM2.5 observations from diplomatic facilities in China. Atmospheric Environment 110, 174–185. https://doi.org/10.1016/j.atmosenv.2015.03.060

Shi, Z., Vu, T., Kotthaus, S., Harrison, R.M., Grimmond, S., Yue, S., Zhu, T., Lee, J., Han, Y., Demuzere, M., Dunmore, R.E., Ren, L., Liu, D., Wang, Y., Wild, O., et al., 2019. Introduction to the special issue "In-depth study of air pollution sources and processes within Beijing and its surrounding region (APHH-Beijing)." Atmospheric Chemistry and Physics 19, 7519–7546. https://doi.org/10.5194/acp-19-7519-2019

Silver, B., Reddington, C.L., Arnold, S.R., Spracklen, D. V, 2018. Substantial changes in air pollution across China during 2015–2017. Environmental Research Letters 13, 114012. https://doi.org/10.1088/1748-9326/aae718

Song, C., He, J., Wu, L., Jin, T., Chen, X., Li, R., Ren, P., Zhang, L., Mao, H., 2017. Health burden attributable to ambient PM2.5 in China. Environmental Pollution 223, 575–586. https://doi.org/10.1016/j.envpol.2017.01.060

Stanaway, J.D., Afshin, A., Gakidou, E., Lim, S.S., Abate, D., Abate, K.H., Abbafati, C., Abbasi, N., Abbastabar, H., Abd-Allah, F., Abdela, J., Abdelalim, A., et al., 2018. Global, regional, and national comparative risk assessment of 84 behavioural, environmental and occupational, and metabolic risks or clusters of risks for 195 countries and territories, 1990–2017: a systematic analysis for the Global Burden of Disease Stu. The Lancet 392, 1923–1994. https://doi.org/10.1016/S0140-6736(18)32225-6

Tian, Y., Jiang, Y., Liu, Q., Xu, D., Zhao, S., He, L., Liu, H., Xu, H., 2019. Temporal and spatial trends in air quality in Beijing. Landscape and Urban Planning 185, 35–43. https://doi.org/10.1016/j.landurbplan.2019.01.006

Turner, M.C., Jerrett, M., Pope, C.A., Krewski, D., Gapstur, S.M., Diver, W.R., Beckerman, B.S., Marshall, J.D., Su, J., Crouse, D.L., Burnett, R.T., 2016. Long-Term Ozone Exposure and Mortality in a Large Prospective Study. American Journal of Respiratory and Critical Care Medicine 193, 1134–1142. https://doi.org/10.1164/rccm.201508-1633OC

Vu, T. V., Shi, Z., Cheng, J., Zhang, Q., He, K., Wang, S., Harrison, R.M., 2019. Assessing the impact of Clean Air Action Plan on Air Quality Trends in Beijing Megacity using a machine learning technique. Atmospheric Chemistry and Physics Discussions 1–18. https://doi.org/10.5194/acp-2019-173

Wang, L., Zhang, F., Pilot, E., Yu, J., Nie, C., Holdaway, J., Yang, L., Li, Y., Wang, W., Vardoulakis, S., Krafft, T., 2018. Taking Action on Air Pollution Control in the Beijing-Tianjin-Hebei (BTH) Region: Progress, Challenges and Opportunities. International Journal of Environmental Research and Public Health 15, 306. https://doi.org/10.3390/ijerph15020306

Wang, N., Lyu, X., Deng, X., Huang, X., Jiang, F., Ding, A., 2019. Aggravating O3 pollution due to NOx emission control in eastern China. Science of The Total Environment 677, 732–744. https://doi.org/10.1016/j.scitotenv.2019.04.388

Wang, T., Nie, W., Gao, J., Xue, L.K., Gao, X.M., Wang, X.F., Qiu, J., Poon, C.N., Meinardi, S., Blake, D., Wang, S.L., Ding, A.J., Chai, F.H., Zhang, Q.Z., Wang, W.X., 2010. Air quality during the 2008 Beijing Olympics: secondary pollutants and regional impact. Atmospheric Chemistry and Physics 10, 7603–7615. https://doi.org/10.5194/acp-10-7603-2010

WB, 2019. World Bank national accounts data, and OECD National Accounts data files. (Available at: https://data.worldbank.org/indicator/NY.GDP.MKTP.CD?locations=CN)

WHO, 2015. WHO Air quality guidelines for particulate matter, ozone, nitrogen dioxide and sulfur dioxide, Global update 2005. Summary of risk assessment. (Available at: https://www.who.int/airpollution/publications/aqg2005/en/)

Wu, Z., Zhang, Y., Zhang, L., Huang, M., Zhong, L., Chen, D., Wang, X., 2019. Trends of outdoor air pollution and the impact on premature mortality in the Pearl River Delta region of southern China during 2006–2015. Science of The Total Environment 690, 248–260. https://doi.org/10.1016/j.scitotenv.2019.06.401

Xiang, J., Weschler, C.J., Zhang, J., Zhang, L., Sun, Z., Duan, X., Zhang, Y., 2019. Ozone in urban China: Impact on mortalities and approaches for establishing indoor guideline concentrations. Indoor Air ina.12565. https://doi.org/10.1111/ina.12565

Xie, Y., Dai, H., Zhang, Y., Wu, Y., Hanaoka, T., Masui, T., 2019. Comparison of health and economic impacts of PM2.5 and ozone pollution in China. Environment International 130, 104881. https://doi.org/10.1016/j.envint.2019.05.075

Yang, Y., Li, R., Li, W., Wang, M., Cao, Y., Wu, Z., Xu, Q., 2013. The Association between Ambient Air Pollution and Daily Mortality in Beijing after the 2008 Olympics: A Time Series Study. PLoS ONE 8, e76759. https://doi.org/10.1371/journal.pone.0076759

Yin, H., Pizzol, M., Xu, L., 2017. External costs of PM2.5 pollution in Beijing, China: Uncertainty analysis of multiple health impacts and costs. Environmental Pollution 226, 356–369. https://doi.org/10.1016/j.envpol.2017.02.029

Zhang, H., Wang, Shuxiao, Hao, J., Wang, X., Wang, Shulan, Chai, F., Li, M., 2016. Air pollution and control action in Beijing. Journal of Cleaner Production 112, 1519–1527. https://doi.org/10.1016/j.jclepro.2015.04.092

Zhang, J., Liu, Y., Cui, L., Liu, S., Yin, X., Li, H., 2017. Ambient air pollution, smog episodes and mortality in Jinan, China. Scientific Reports 7, 11209. https://doi.org/10.1038/s41598-017-11338-2

Zhang, Q., Zheng, Y., Tong, D., Shao, M., Wang, S., Zhang, Y., Xu, X., Wang, J., He, H., Liu, W., Ding, Y., Lei, Y., Li, J., Wang, Z., Zhang, X., Wang, Y., Cheng, J., Liu, Y., Shi, Q., Yan, L., Geng, G., Hong, C., Li, M., Liu, F., Zheng, B., Cao, J., Ding, A., Gao, J., Fu, Q., Huo, J., Liu, B., Liu, Z., Yang, F., He, K., Hao, J., 2019. Drivers of improved PM 2.5 air quality in China from 2013 to 2017. Proceedings of the National Academy of Sciences 116, 24463–24469. https://doi.org/10.1073/pnas.1907956116

Zhang, X., Xu, X., Ding, Y., Liu, Y., Zhang, H., Wang, Y., Zhong, J., 2019. The impact of meteorological changes from 2013 to 2017 on PM2.5 mass reduction in key regions in China. Science China Earth Sciences. https://doi.org/10.1007/s11430-019-9343-3

Zhang, X., Ou, X., Yang, X., Qi, T., Nam, K.-M., Zhang, D., Zhang, Xiliang, 2017. Socioeconomic burden of air pollution in China: Province-level analysis based on energy economic model. Energy Economics 68, 478–489. https://doi.org/10.1016/j.eneco.2017.10.013

Zhang, Y.-L., Cao, F., 2015. Fine particulate matter (PM2.5) in China at a city level. Scientific Reports 5, 14884. https://doi.org/10.1038/srep14884

Zhang, Z., Ma, Z., Kim, S.-J., 2018. Significant Decrease of PM2.5 in Beijing Based on Long-Term Records and Kolmogorov–Zurbenko Filter Approach. Aerosol and Air Quality Research 18, 711–718. https://doi.org/10.4209/aaqr.2017.01.0011

Zhu, G., Hu, W., Liu, Y., Cao, J., Ma, Z., Deng, Y., Sabel, C.E., Wang, H., 2019. Health burdens of ambient PM2.5 pollution across Chinese cities during 2006–2015. Journal of Environmental Management 243, 250–256. https://doi.org/10.1016/j.jenvman.2019.04.119

Table 1. Annual average pollution concentrations from 2014 to 2018 in four typical sites in Beijing (US, SUB, RBS and TS represent the urban site, the sub-urban site, the regional background site and the traffic site; concentration unit is in μg/m^3)

	Sites	2014	2015	2016	2017	2018
$PM_{2.5}$	US	89.8±81.5	83.1±83.2	74.5±72.4	60.3±63.9	52.4±49.0
	SUB	88.5±77.4	80.5±76.1	70.6±66.4	59.0±59.3	50.6±46.6
	RBS	89.3±75.3	81.1±72.0	74.7±64.6	60.3±56.1	56.1±47.0
	TS	98.6±89.0	90.5±91.4	80.7±79.1	65.5±68.7	55.3±52.5
O_3	US	112.8±65.8	99.6±65.7	97.3±63.4	97.7±60.1	103.3 ±59.6
	SUB	115.0±63.5	99.9±62.9	100.9±62.4	104.1± 61.8	105.4± 60.9
	RBS	117.0±62.6	102.0±62.2	101.4±59.2	97.8±53.4	103.8±54.5
	TS	83.6±50.3	76.8±51.3	78.6±52.4	79.8±52.9	82.8±50.5
NO_2	US	55.9±30.8	52.2±30.9	51.3±30.0	48.1±28.0	43.6± 26.2
	SUB	45.1±24.2	43.5±25.6	42.8±25.4	42.0±23.6	37.5± 21.5
	RBS	37.9±19.8	37.1±21.6	37.1±20.8	34.9±18.1	32.5±17.6
	TS	82.1±32.7	75.7±33.3	69.8±31.4	67.2±30.2	64.4±28.7
SO_2	US	13.7±12.9	14.0±14.6	10.5±10.6	8.1±8.8	5.9±4.0
	SUB	12.3 ±12.0	13.4±14.1	10.7±10.2	8.6±8.7	6.0±4.0
	RBS	14.9±11.0	13.4±13.1	10.6±9.2	8.9±8.0	6.3±4.6
	TS	16.0±14.0	17.5±17.0	13.9±12.0	6.3±5.2	7.6±4.9

Table 2. Cause-specific premature deaths attributed to $PM_{2.5}$ and O_3 in 16 districts in Beijing

	2014						2018					
	$PM_{2.5}$					O_3	$PM_{2.5}$					O_3
Districts	IHD	Stroke	COPD	LC	ALRI	Non-accidental	IHD	Stroke	COPD	LC	ALRI	Non-accidental
Daxing	787	1032	180	156	4	205	874	1145	154	134	4	173
Mentougou	150	198	30	26	1	72	154	200	25	22	1	59
Haidian	1832	2410	387	334	9	392	1687	2197	284	246	6	233
Miyun	232	305	45	39	1	172	232	299	37	32	1	151
Yanqing	153	201	29	26	1	71	162	209	26	22	1	42
Huairou	187	246	37	33	1	98	192	247	31	26	1	52
Pinggu	208	274	42	37	1	102	217	283	37	32	1	110
Shijingshan	324	426	68	60	2	104	299	390	52	44	1	100
Fengtai	1161	1524	258	220	6	213	1067	1392	185	159	4	156
Dongcheng	458	602	100	86	2	173	417	545	72	62	2	137
Shunyi	499	656	103	90	2	212	547	712	92	80	2	208
Fangshan	532	696	125	108	3	141	580	759	107	91	2	189
Chaoyang	1967	2580	422	366	10	406	1812	2361	306	265	7	299
Xicheng	651	855	137	120	3	283	591	770	100	86	2	194
Changping	934	1228	187	160	4	231	978	1259	157	135	3	178
Tongzhou	693	908	161	138	4	158	754	989	136	119	3	191

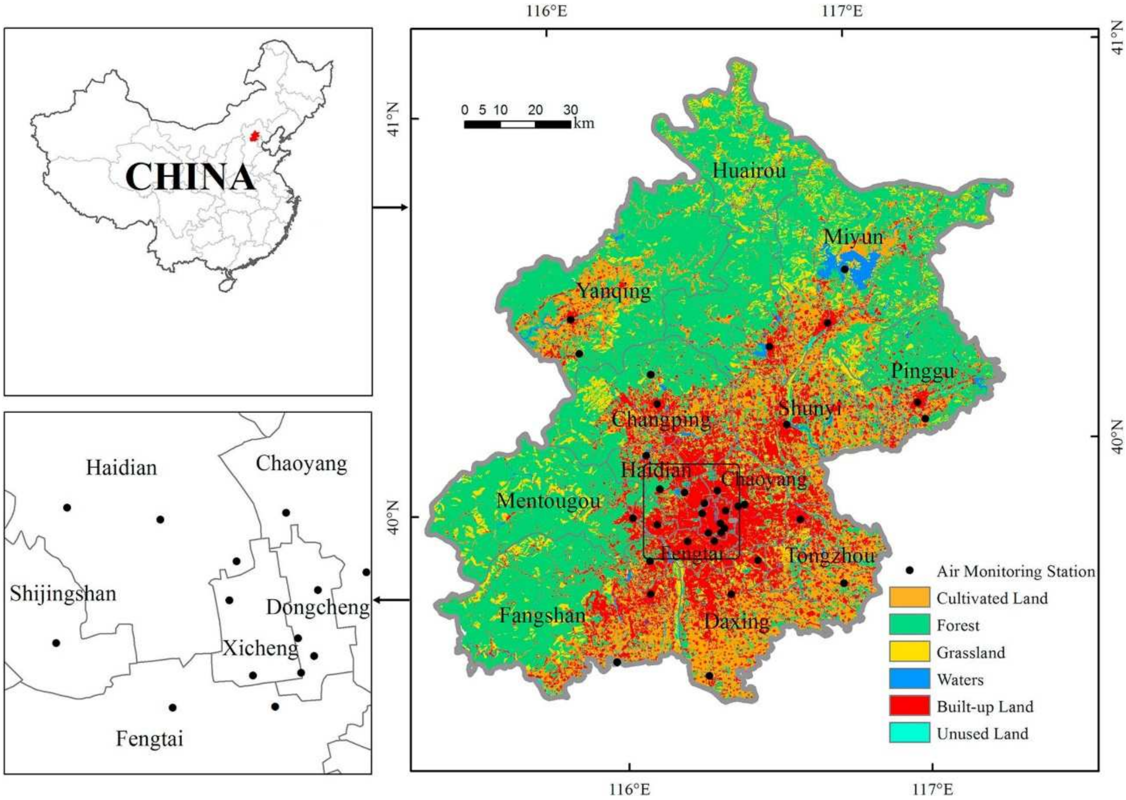

Fig. 1. Location of the 35 air quality monitoring sites in Beijing (Tian et al., 2019)

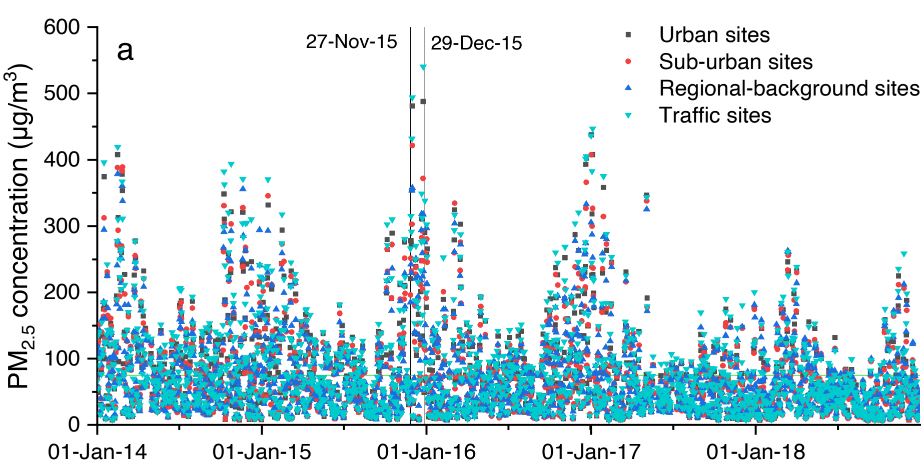

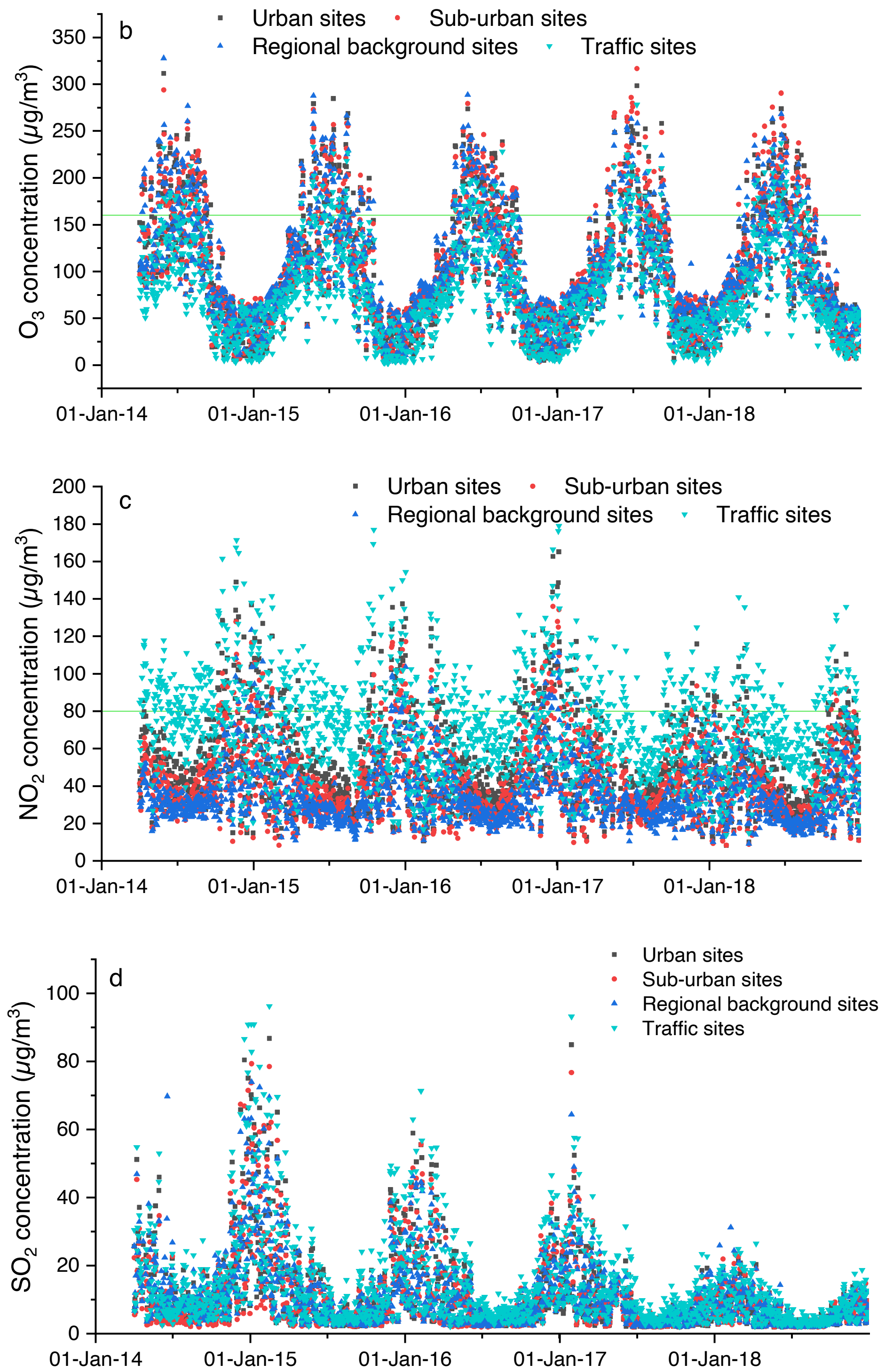

Fig. 2. Daily average pollution concentrations (a: $PM_{2.5}$; b: MDA8-h O_3; c: NO_2; d: SO_2) at the four typical sites in Beijing from 2014 to 2018. (units are $\mu g/m^3$) ($PM_{2.5}$ extreme events shown in the box and green horizontal line indicating the Grade II standard).

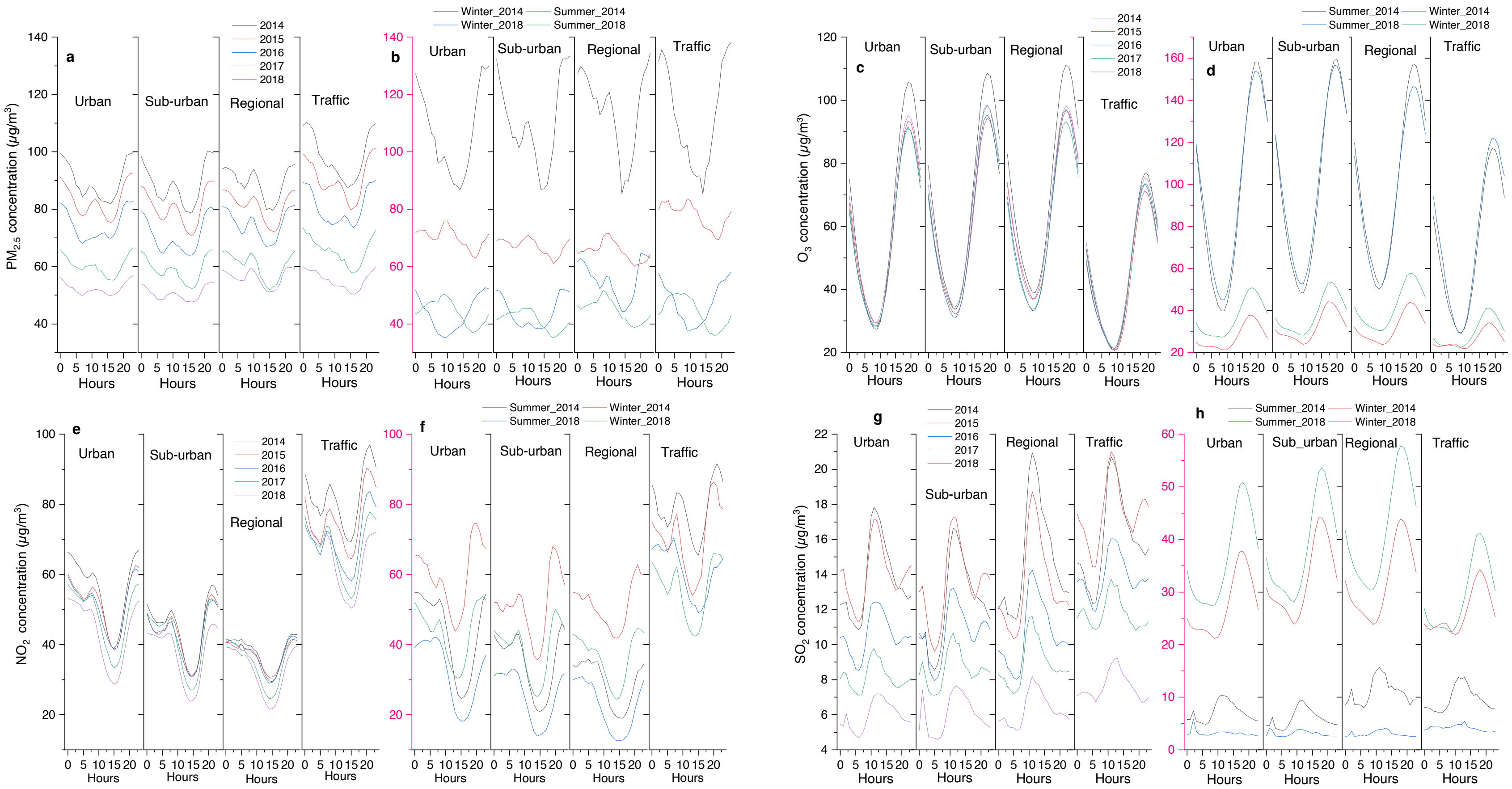

Fig. 3. Diurnal variations of $PM_{2.5}$ (a and b), O_3 (c and d), NO_2 (e and f) and SO_2 (g and h) at four typical sites in Beijing. (a, c, e and g for yearly average, and b, d, f and h for the seasonal summer and winter variations in 2014 and 2018)

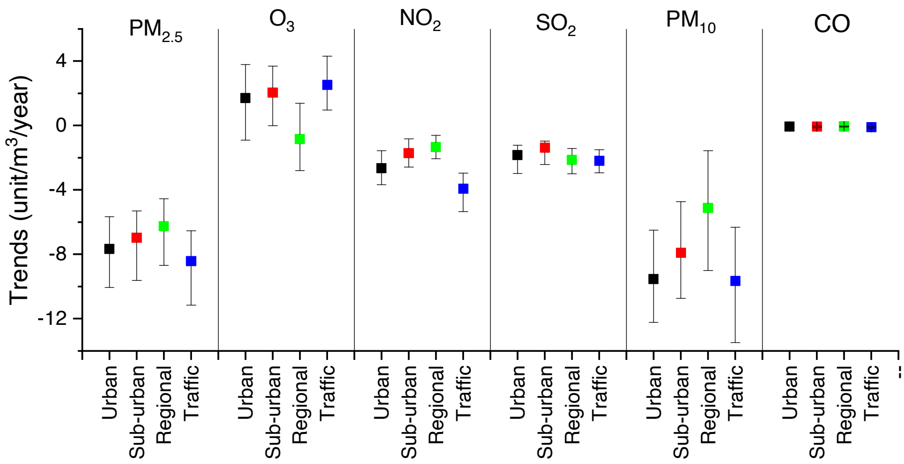

Fig. 4. The trends of pollutants from 2014 to 2018 (mean values with error bars represent 95% confidence intervals; the unit for the trends is μg/m^3/year for $PM_{2.5}$, O_3, NO_2, SO_2 and PM_{10}, and mg/m^3/year for CO).

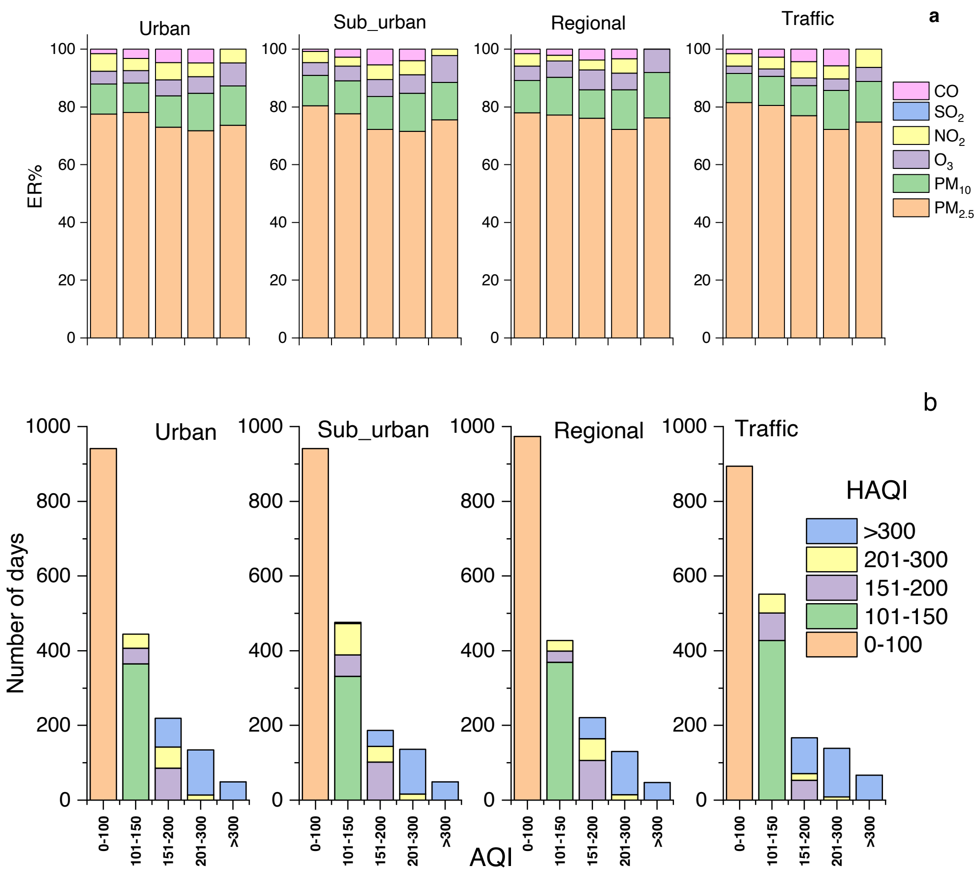

Fig. 5. (a) Percentage of excess risk of the pollutants from 2014 to 2018. (b) Comparison of the HAQI-classified health risk categories with the AQI-classified categories (with the average number of days in different ranges; the sum of all year data was included in the analysis).

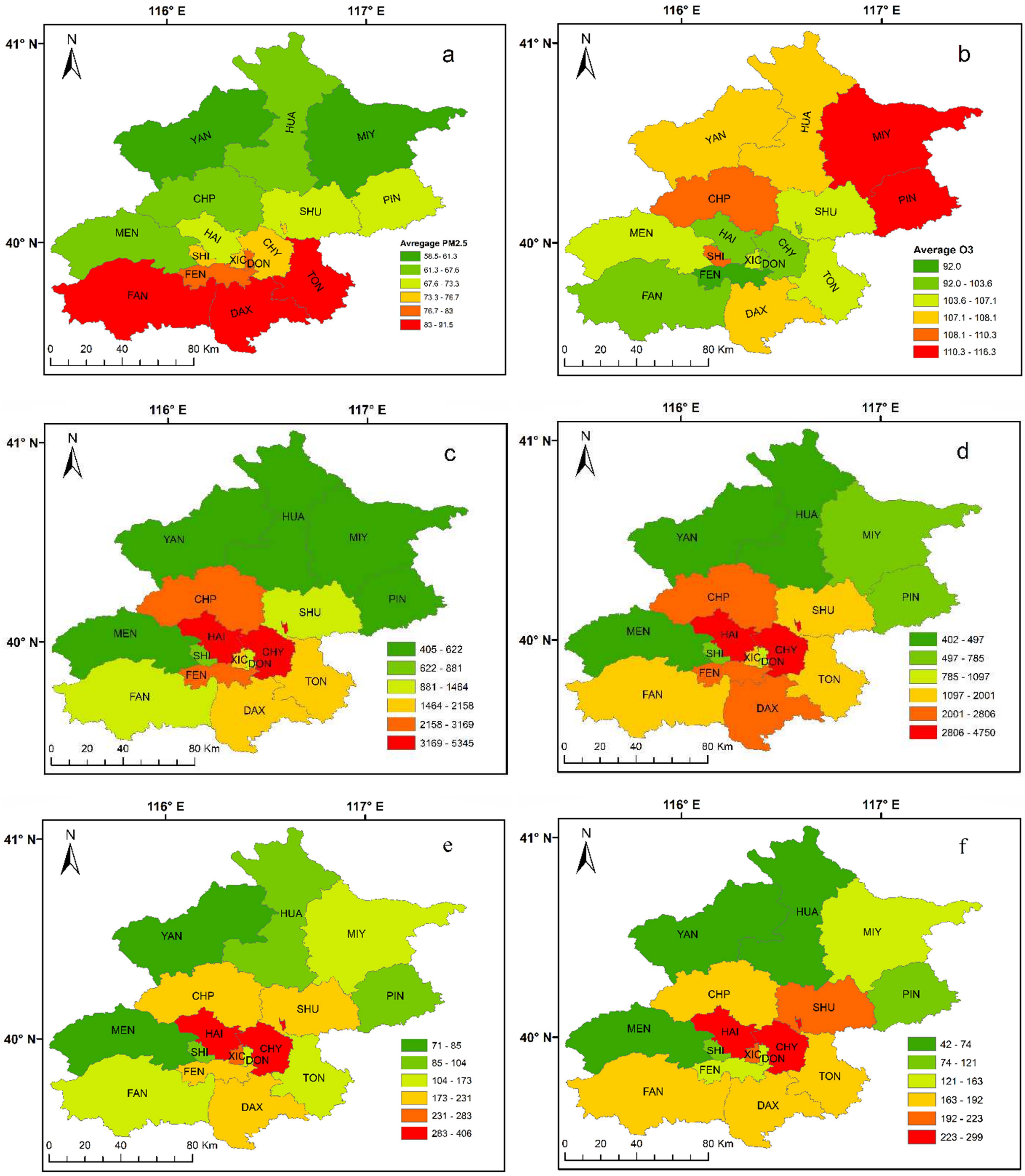

Fig. 6. District-specific (a) annual average $PM_{2.5}$ concentration ($\mu g/m^3$), (b) annual average O_3 concentration ($\mu g/m^3$) in Beijing from 2014 to 2018, $PM_{2.5}$-attributed premature mortality for the year (c) 2014 and (d) 2018, and O_3-attributed premature mortality for the year (c) 2014 and (d) 2018.

Note: DAX, MEN, HAI, MIY, YAN, HUA, PIN, SHI, FEN, DON, SHU, FAN, CHA, XIC, CHA and TON refer to the districts of Daxing, Mentougou, Haidian, Miyun, Yanqing, Huairou, Pinggu, Shijingshan, Fengtai, Dongcheng, Shunyi, Fangshan, Chaoyang, Xicheng, Changping and Tongzhou